# *High-strength, healable, supramolecular polymer nanocomposites*

Article

Supplemental Material

## Supporting Information

# High-Strength, Healable, Supramolecular Polymer Nanocomposites

Justin Fox,[1] Jeong J. Wie,[2] Barnaby W. Greenland,[3] Stefano Burattini,[3] Wayne Hayes,[3] Howard M. Colquhoun,[3] Michael E. Mackay,[2,4]* and Stuart J. Rowan,[1]*

[1] *Department of Macromolecular Science and Engineering, 2100 Adelbert Road, Kent Hale Smith Building, Cleveland, Ohio 44106, USA.*

[2] *Department of Chemical Engineering, University of Delaware, 150 Academy St., Newark, DE, 19716, USA.*

[3] *Department of Chemistry, University of Reading, Whiteknights, Reading, RG6 6AD, UK.*

[4] *Department of Materials Science & Engineering, University of Delaware, 201 DuPont Hall, Newark, DE, 19716, USA.*

## Contents

**Isolation and characterization of CNCs**

Tunicates (*Styela clava*) were collected from Snug Harbor Marina (Wakefield, RI) and processed into cellulose nanocrystals (CNCs) as previously described.[1] TEM images of CNCs were acquired using a JEOL 1200EX Transmission Electron Microscope. All samples were prepared on carbon-coated copper grids using a standard uranyl acetate negative staining method.[2] Conductometric titrations were conducted on an Accumet AR50 Dual Channel pH/Ion/Conductivity Meter using established techniques.[3]

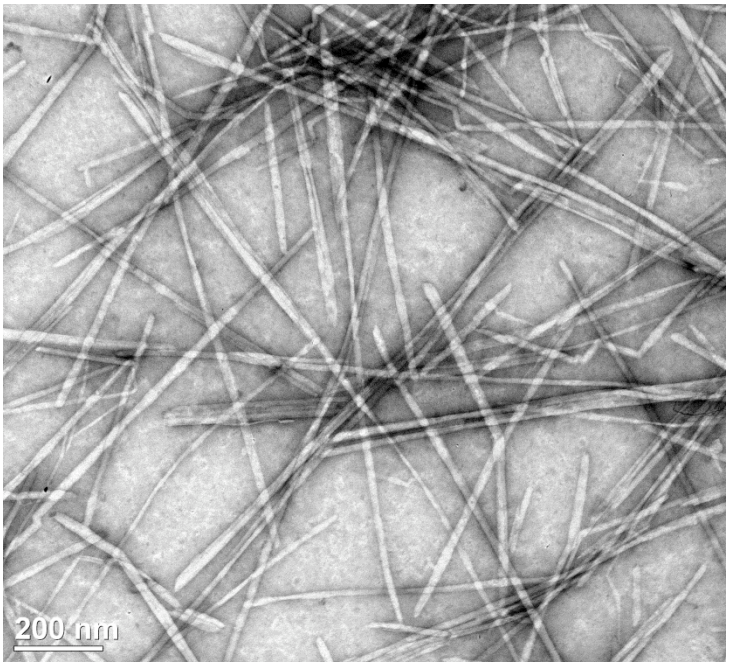


**Figure S1. Transmission electron microscopy of tunicate whiskers**, as isolated from tunicate mantles.

**Conductometric titration of CNCs**

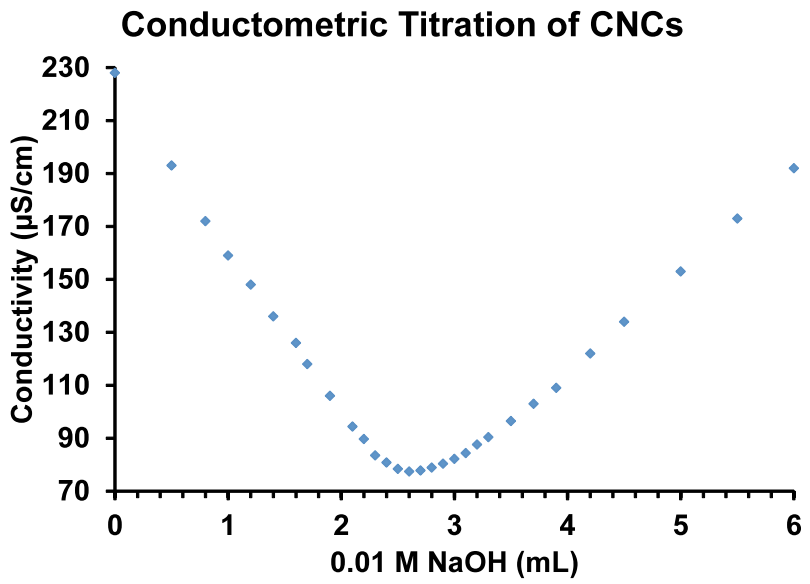


**Figure S2. Conductometric Titration of CNCs.** Typical curve representing conductometric titration of 50 mg of CNCs suspended in approx. 50 mL of deionized $H_2O$. Three titrations are performed and averaged to yield sulfate charge density of 130 mmol/kg for the CNCs used in this study.

**Thermogravimetric analysis**

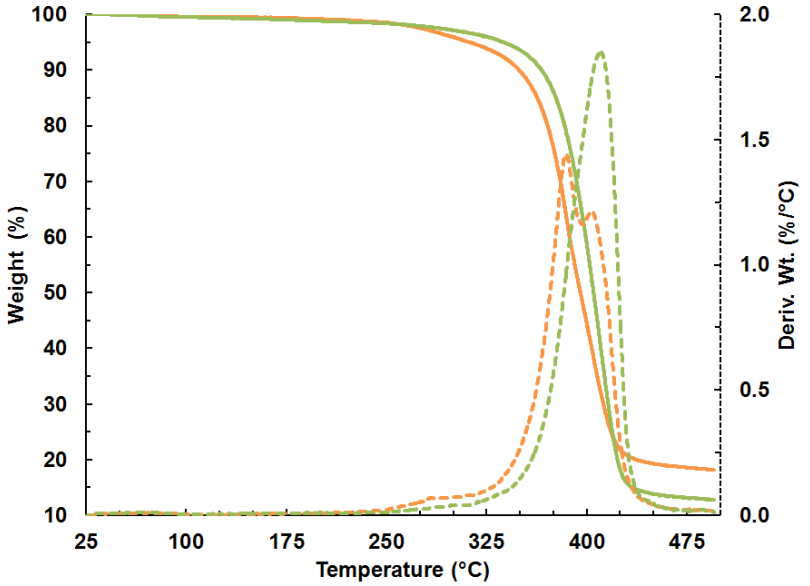


**Figure S3. TGA of typical nanocomposite.** Typical weight loss curves (solid lines) for dried nanocomposites of 5 wt.% CNC (green) and 20 wt. % CNC (orange). Derivative weight loss given as green and orange dashed lines (for 5 and 20 wt.%, respectively) and correspond with dashed axis on right.

**Effects of Compression Molding**

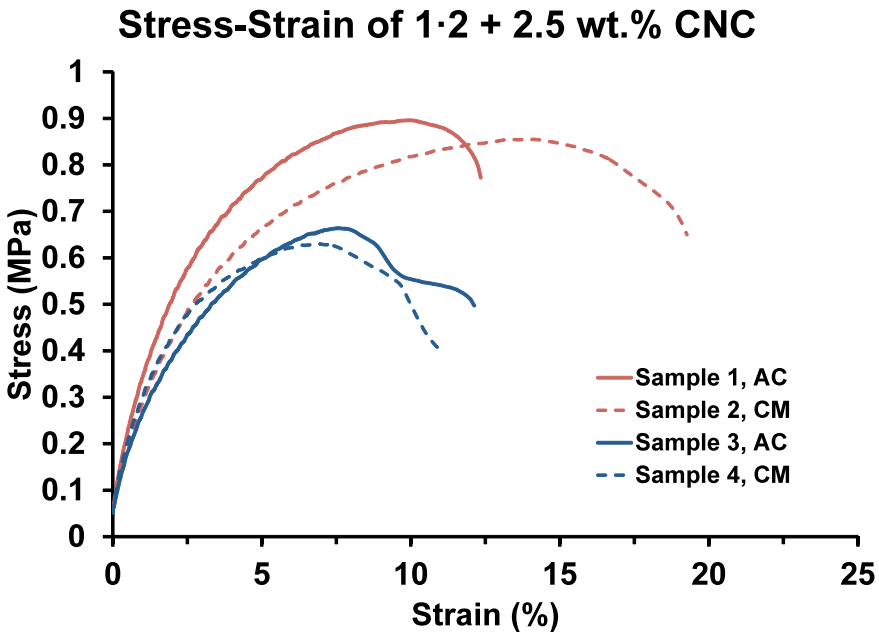


**Figure S4. Stress-Strain curves for typical nanocomposites.** Samples of **1·2** + 2.50 wt.% CNC were subject to tensile testing in their as-cast state (AC, solid lines) and after compression molding at 85 °C under 200 kPa for 5 minutes (CM, dashed lines). Samples represented by lines of the same color were cut from adjacent areas of film. Compression molded samples have more consistent tensile moduli, indicated by the near superposition of the data representing Samples 2 and 4 below 2.5 % strain.

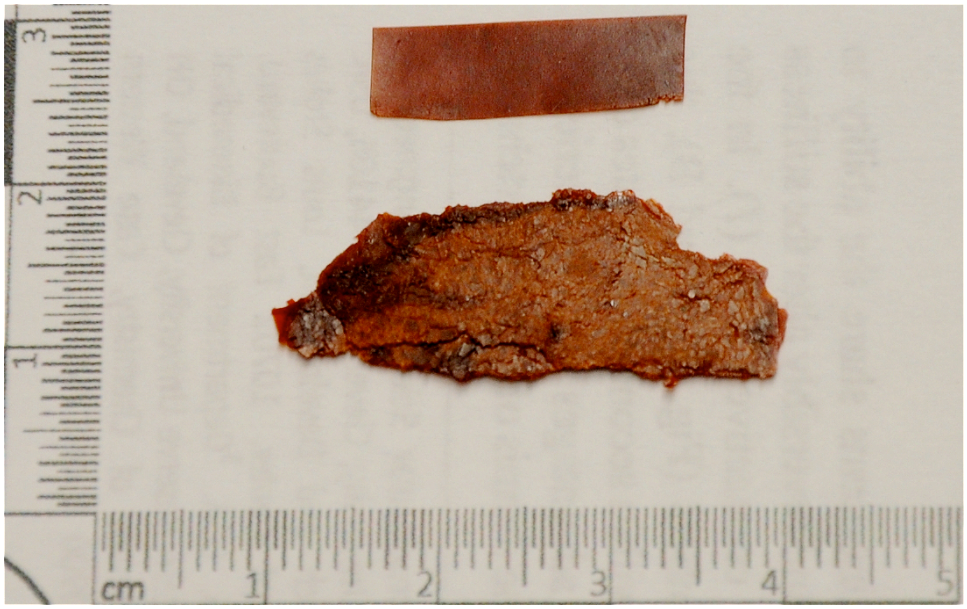


**Figure S5.** Image of 20 wt.% nanocomposite films as cast from solution (top sample) and after melt processing at 85 °C and 200 kPa (bottom sample).

## Rheology Data

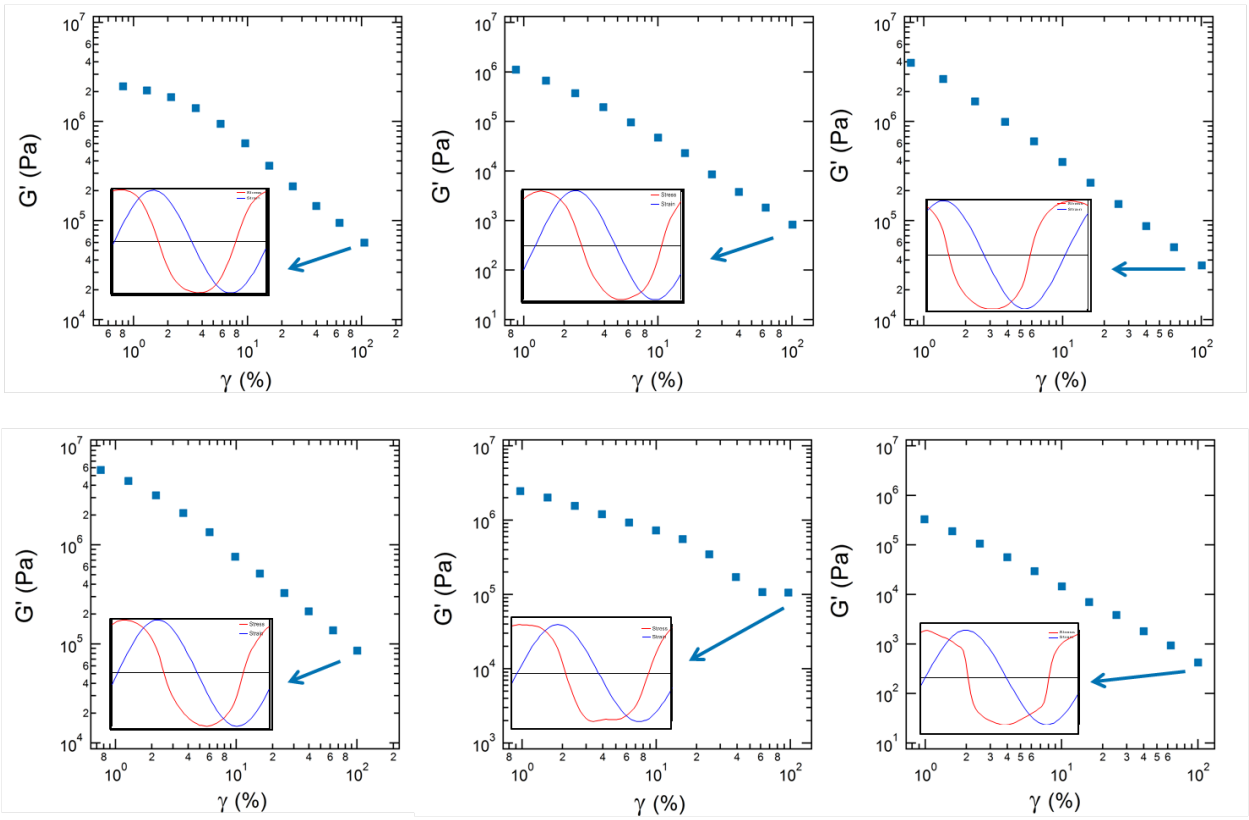


**Figure S6. Deformation process for 1.25 wt.%, 2.50 wt.% and 5.00 wt.% (top left to right) and 7.50 wt.%, 10.00 wt.% and 20.00 (bottom left to right) at 65°C. Frequency of ω=100 rad/s was applied to 1.25 wt.% and 2.50 wt.% nanocomposites and ω=10 rad/s was applied to 5.00 wt.%, 7.50 wt.%, 10.00 wt.% and 20.00 wt.% nanocomposites.**

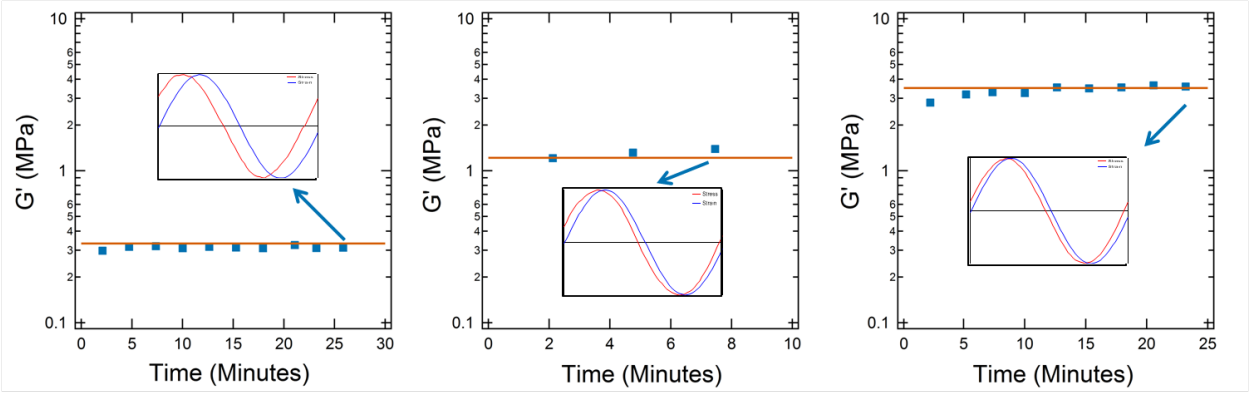


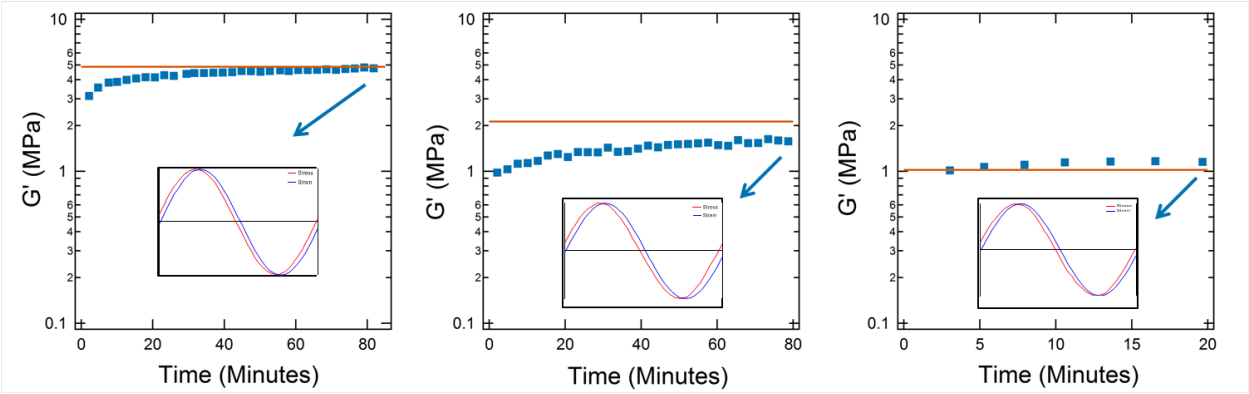


**Figure S7. Rate of recovery (ω=0.1 rad/s, γ=0.1 %) of 1.25 wt.%, 2.50 wt.%, 5.00 wt.%, (top left to right) 7.50 wt.%, 10.00 wt.% and 20.00 wt.% (bottom left to right) nanocomposites at 65°C.** The initial modulus (red line) was measured at 65°C at low frequency and strain (ω=0.1 rad/s, γ=0.1%). The samples were then broken using a strain sweep as shown in Figure S6. Recovery of the shear storage modulus was then monitored at 65°C over a period of time (ω=0.1 rad/s, γ=0.1 %)

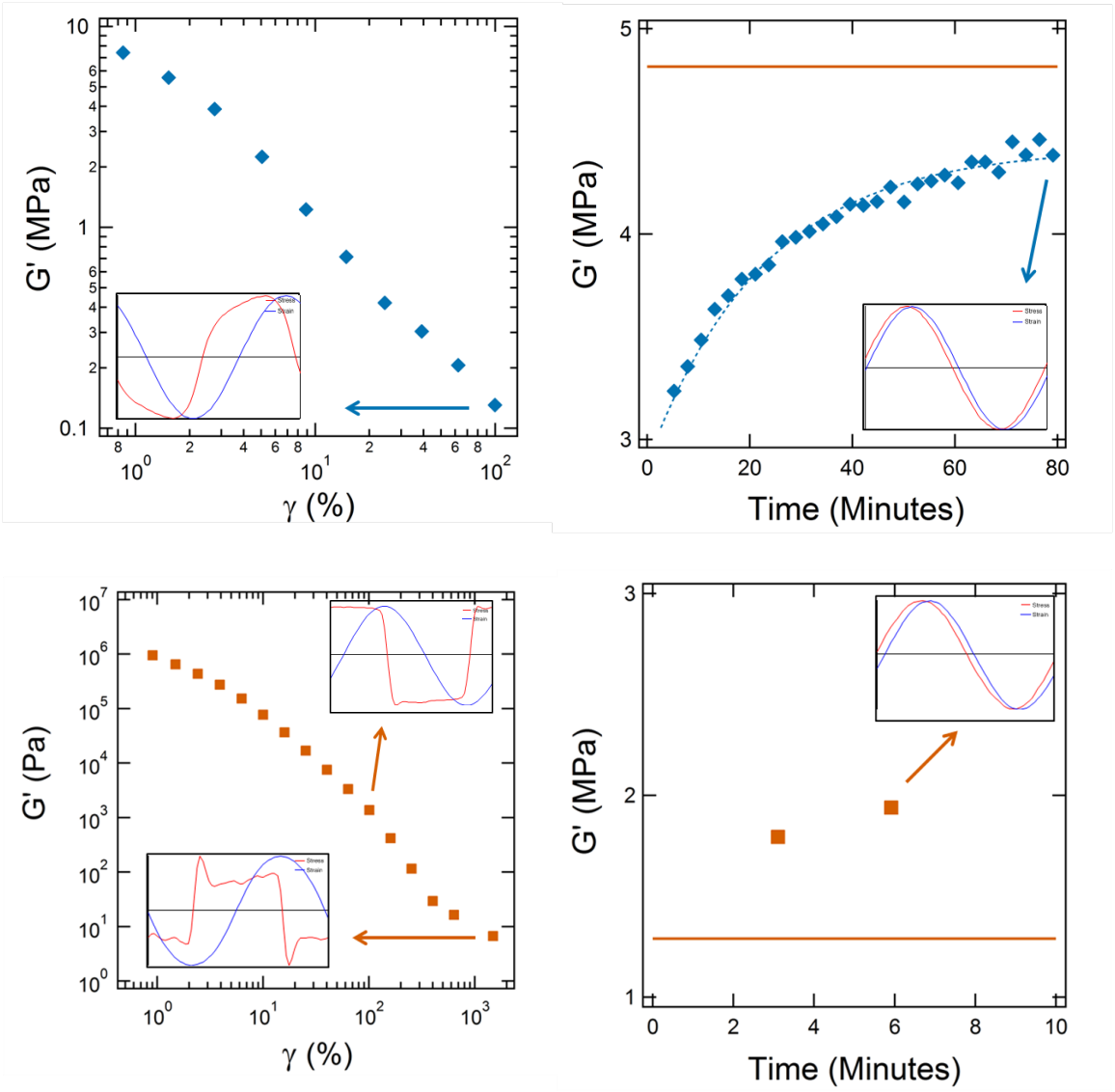


**Figure S8. Deformation process, left, (ω=100 rad/s) and rate of recovery, right, (ω=0.1 rad/s, γ=0.1 %) of 7.50 wt.% (top) and 20.00 wt.% (bottom) nanocomposite at 65°C.** The initial modulus (red line) was measured at 65°C at low frequency and strain (ω=0.1 rad/s, γ=0.1%). The sample was then broken using a strain sweep (ω=100 rad/s). Recovery of the shear storage modulus was then monitored at 65°C over a period of time (ω=0.1 rad/s, γ=0.1 %)

As previously shown in Figure S7, after experiencing the deformation process at a frequency of 10 rad/s, the 7.50 wt% nanocomposite fully recovered its initial modulus at the 80 minute time mark. However, the same sample deformed at 100 rad/s only recovered about 90% of the initial modulus at the same time mark as shown in Figure S8. Non-linear and linear stress-strain responses were observed for the deformed and the self-healed nanocomposites, respectively. Deformed 20.00 wt.% nanocomposite showed the highly non-linear stress-strain response at 100 rad/s and 1000% of strain. The linear stress-strain response was recovered only within 3 minutes of self-healing process at 65 °C. The recovered modulus was even higher than the initial modulus, once again providing evidence for phase separation of 20.00 wt.% nanocomposite. It

appears that high shear and strain helped the mixing of phase-separated whiskers in the polymer matrix and increased storage modulus. After the self-healing process, all the nanocomposites studied recovered the linear stress-strain responses.

## Electron microscopy studies

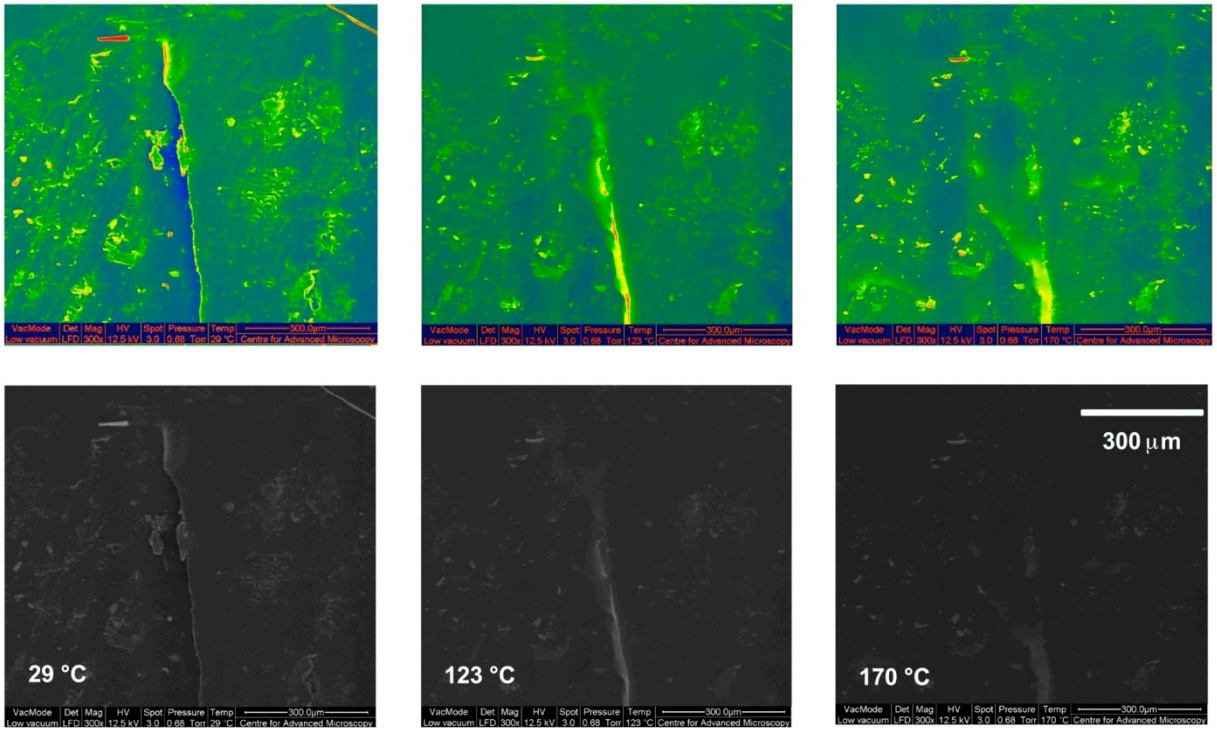


**Figure S9. Healing of the 1.25wt% CNC composite.** The sample was fractured and then heated to 200 °C, at 5 °C $min^{-1}$, in an environmental scanning electron microscope (FEI Quanta FEG 600). The images show progressive healing of the sample between room temperature and 170 °C. Original micrographs are reproduced below, with corresponding false-color images above.

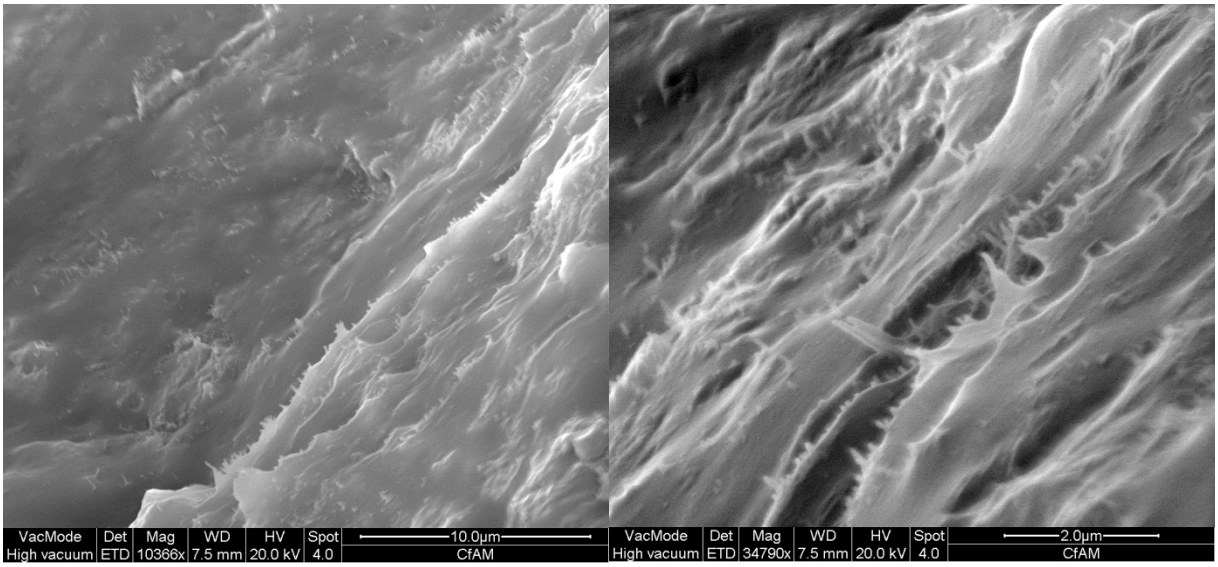


**Figure S10: SEM images of the fracture surface of the 7.5 wt% composite.** SEM images were acquired on a FEI Quanta field-emission scanning electron microscope at an accelerating voltage of 20 kV.

## References

[1] van den Berg, O.; Capadona, J. R.; Weder, C. *Biomacromolecules* **2007**, *8*, 1353-1357.
[2] le Cam, E.; Frechon, D.; Barray, M.; Fourcade, A.; Delain, E. *Proc. Natl. Acad. Sci. USA* **1994**, *91*, 11816-11820.
[3] Rusli, R.; Shanmuganathan, K.; Rowan, S. J.; Weder, C.; Eichhorn, S. J. *Biomacromolecules*, **2011,** *12*, 1363-1369.